The Volcanic Signal in Goddard Institute for Space Studies Three-Dimensional Model Simulations

ALAN ROBOCK AND YUHE LIU

Department of Meteorology, University of Maryland, College Park, Maryland

(Manuscript received 18 October 1992, in final form 29 June 1993)

ABSTRACT

Transient calculations of the Goddard Institute for Space Studies general circulation model for the climatic signal of volcanic eruptions are analyzed. By compositing the output for two different volcanoes for scenario A and five different volcanoes for scenario B, the natural variability is suppresssed and the volcanic signals are extracted.

Significant global mean surface air temperature cooling and precipitation reduction are found for several years following the eruptions, with larger changes in the Northern Hemisphere (NH) than in the Southern Hemisphere. The global-average temperature response lasts for more than four years, but the precipitation response disappears after three years. The largest cooling in the model occurs in the NH summer of the year after spring eruptions. Significant zonal-average temperature reductions begin in the tropics immediately after the eruptions and extend to 45°S–45°N in the year after the eruptions. In the second year, cooling is still seen from 30°S to 30°N. Because of the low variability in this model as compared to the real world, these signals may appear more significant here than they would by attempting to isolate them using real data. The results suggest that volcanoes can enhance the drought in the Sahel. No evidence was found that stratospheric aerosols from the low-latitude volcanic eruptions can trigger ENSO events in this model.

1. Introduction

Benjamin Franklin (1784) was the first to point out that emissions from volcanoes might be a possible cause of weather and climate variations when he suggested that the Laki eruption in Iceland in 1783 might have been responsible for the abnormally cold winter of 1783–84. There have been many studies since then that show that volcanoes can be important causes of hemispheric temperature changes for several years following large eruptions, and on a 100-yr time scale when their cumulative effects are taken into account, but the results differ on many details, and a generally accepted theory of the response of the climate system to volcanoes (beyond cooling at the surface and warming in the stratosphere) does not exist.

The current state of knowledge of the effect of volcanoes on climate is represented in the reviews of Lamb (1970), Toon and Pollack (1980), Toon (1982), Ellsaesser (1983), Asaturov et al. (1986), Kondratyev (1988), and Robock (1991). Volcanic eruptions that inject large amounts of sulfur-rich gas into the stratosphere produce dust veils that last several years and cool the earth's surface. At the same time, these dust veils absorb enough longwave and solar radiation to warm the stratosphere. Since these temperature changes at the earth's surface and in the stratosphere are both in the opposite direction of hypothesized effects from greenhouse gases, they can act to delay and mask the detection of greenhouse effects on the climate system.

In order to better understand the volcanic impact on climate, we would like to know the spatial and temporal pattern of response of the climate system to aerosol particles produced from volcanic eruptions. On the time scale of years, is there a preferential time of year or latitude of the climatic response? Do the land and ocean both show a signal, and how do they compare? Are there significant responses in variables other than temperature? On the time scale of months, is there a strong signal? What will be the effect of the June 1991 Mt. Pinatubo eruption on climate?

There are several causes of climate change on the time scale of months to a few years. If one examines data to try to extract the signal of volcanic eruptions, it is necessary, but difficult, to separate out the signals of greenhouse warming, El Niño–Southern Oscillation (ENSO), and random variations, as shown by Robock and Mao (1992, 1994) in companion papers. The problems include not knowing when major eruptions occurred in the past, and not knowing how to decompose ENSO and volcanic signals in the tropics when they may involve nonlinear interactions in the climate system. In order to avoid these problems, in this paper we utilize general circulation model (GCM) calcula-

Corresponding author address: Prof. Alan Robock, Department of Meteorology, University of Maryland, College Park, MD 20742-2425.

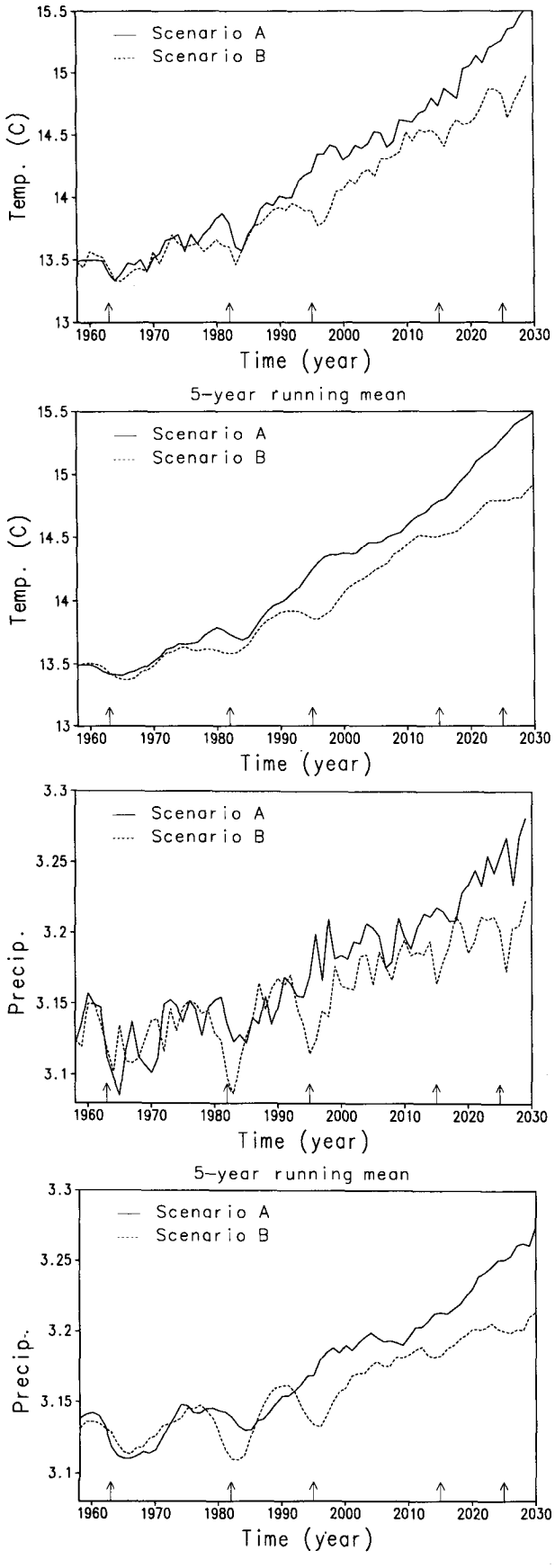

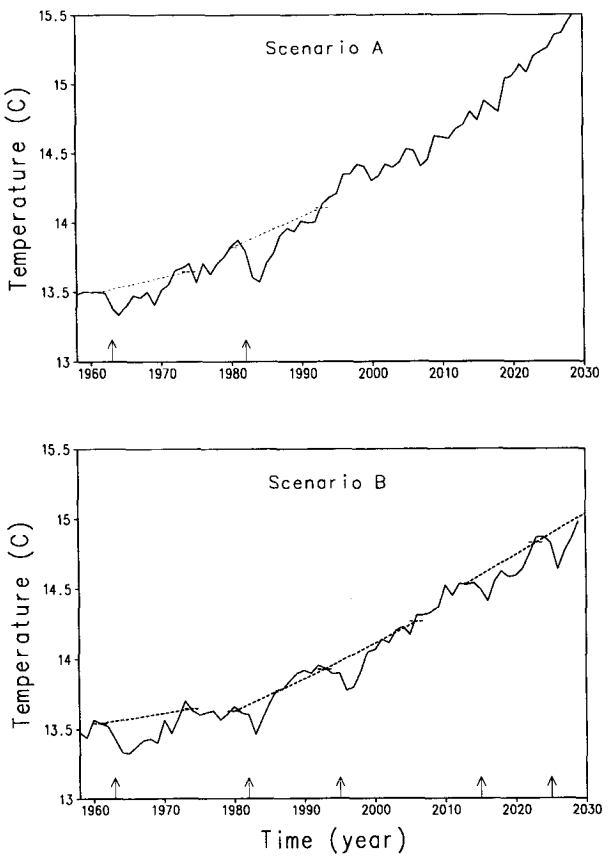

FIG. 2. Illustration of the procedure for extraction of the volcanic signal for the temperature from the transient runs. The difference between the dashed lines and the solid lines was used for each volcano as the volcanic anomaly.

tions that were made to simulate the transient evolution of future climate as a surrogate climatic time series. However, in this case, there are no ENSO events and we know precisely the forcing that was applied.

Another way to look at this work is in the context of the "detection problem." In order to detect the signal of anthropogenic warming in the climate system, it is necessary to characterize the specific signal that is being sought as well as the signals of all other potential forcings. This is so that the other signals can be removed to more clearly see the signal being sought. One of the most important such signals is that of volcanic eruptions, as discussed above. Thus, here we attempt to extract and characterize the volcanic signal from a GCM calculation both to determine its pattern and as

FIG. 1. Annual average, global average temperature (° C) and precipitation (mm day $^{-1}$) from scenarios A and B of the transient GCM calculations of Hansen et al. (1988). The five volcanoes are indicated by arrows. The first two volcanoes were used as forcing for scenario A and all five were used for scenario B.

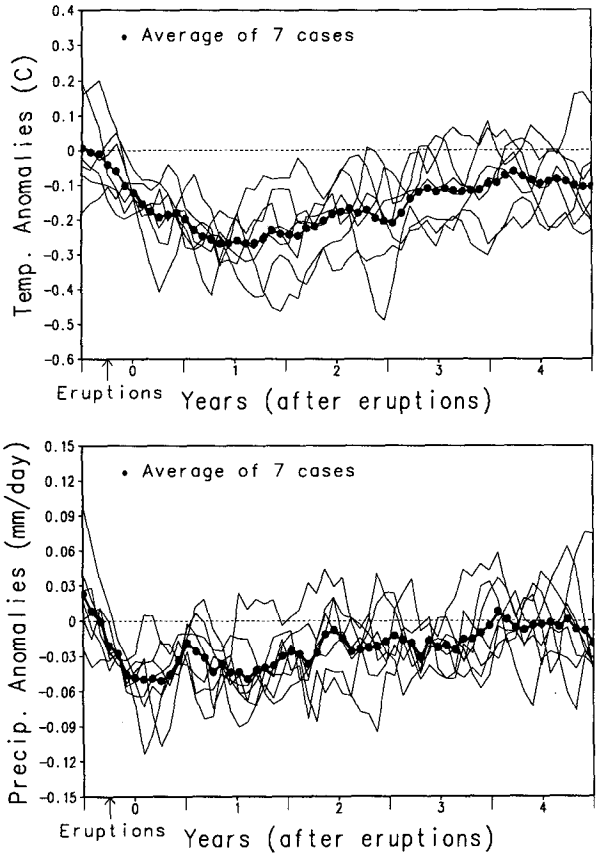

FIG. 3. Global mean anomalies of temperature and precipitation for each of the seven volcano cases and for the average of the cases. For this figure and Figs. 4–7, numbers on the abscissa are at the midpoints of the years and vertical lines indicate divisions between years. Eruptions occurred in the spring of year 0.

a pilot project for the more difficult job of doing the same thing with actual data.

Only a few GCM calculations have been performed to look at the effects of volcanic eruptions. Hunt (1977) presented the first GCM calculation of the effects of a volcano on climate, but it was done with a crude model covering only one hemisphere. In his calculation a cooling response of 0.3°C in hemispheric mean surface temperature was obtained while the cooling in the tropics was about 0.7°C, but he excluded seasonal effects, orography, and ocean thermal inertia. He pointed out that at high latitudes the signals of volcanic aerosols tended to be masked by the "local weather variation." In spite of the limitations of his study, all these results are confirmed here. Rind et al. (1992) presented a calculation with the NASA Goddard Institute for Space Sciences (GISS) Climate/Middle Atmosphere Model on the impact of volcanic aerosols. They found cooling in the troposphere but used fixed boundary conditions from another simulation (actually Pollack et al. 1993) and so did not examine the time-dependent surface response. Graf et al. (1992) looked at the *tropospheric* forcing from volcanic aerosols using forcings as described by Hirono (1988) with the Max-Planck-Institut ECHAM1 GCM and found various patterns of temperature response depending on the distribution of the forcing, but these responses would be short lived, as the lifetime of the tropospheric aerosols would be less than 1 month. Recently Graf et al. (1994) used the ECHAM2 model to examine the Northern Hemisphere (NH) winter response to stratospheric aerosols with a perpetual January experiment and found distinct warming over the NH high-latitude continents.

Hansen et al. (1988) is the only calculation that has included long-term effects of transient volcanic eruptions. They performed time-dependent simulations of climate from 1960 through 2050 with the GISS GCM. In three different simulations with different amounts of greenhouse gases, the effects of a total of 12 large and 9 small volcanoes were shown to cause cooling for several years. Although Hansen et al. presented annual-average temperature results of these simulations, showing cooling from the volcanoes, the seasonal and latitudinal temperature signal and the precipitation or wind signals of the volcanoes were not analyzed in their output. In addition, the simple ocean model used pre-

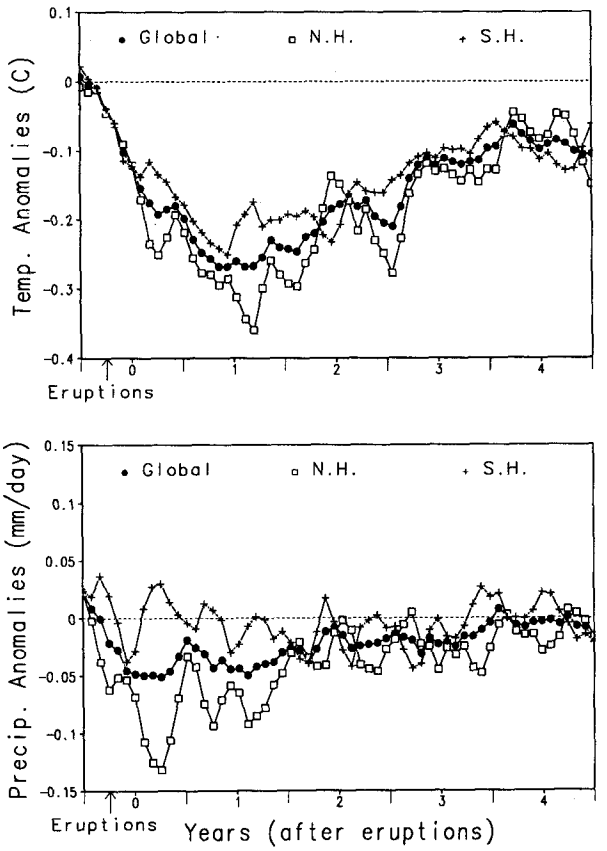

FIG. 4. Global mean and hemispheric mean anomalies of temperature and precipitation for the average of the seven volcano cases.

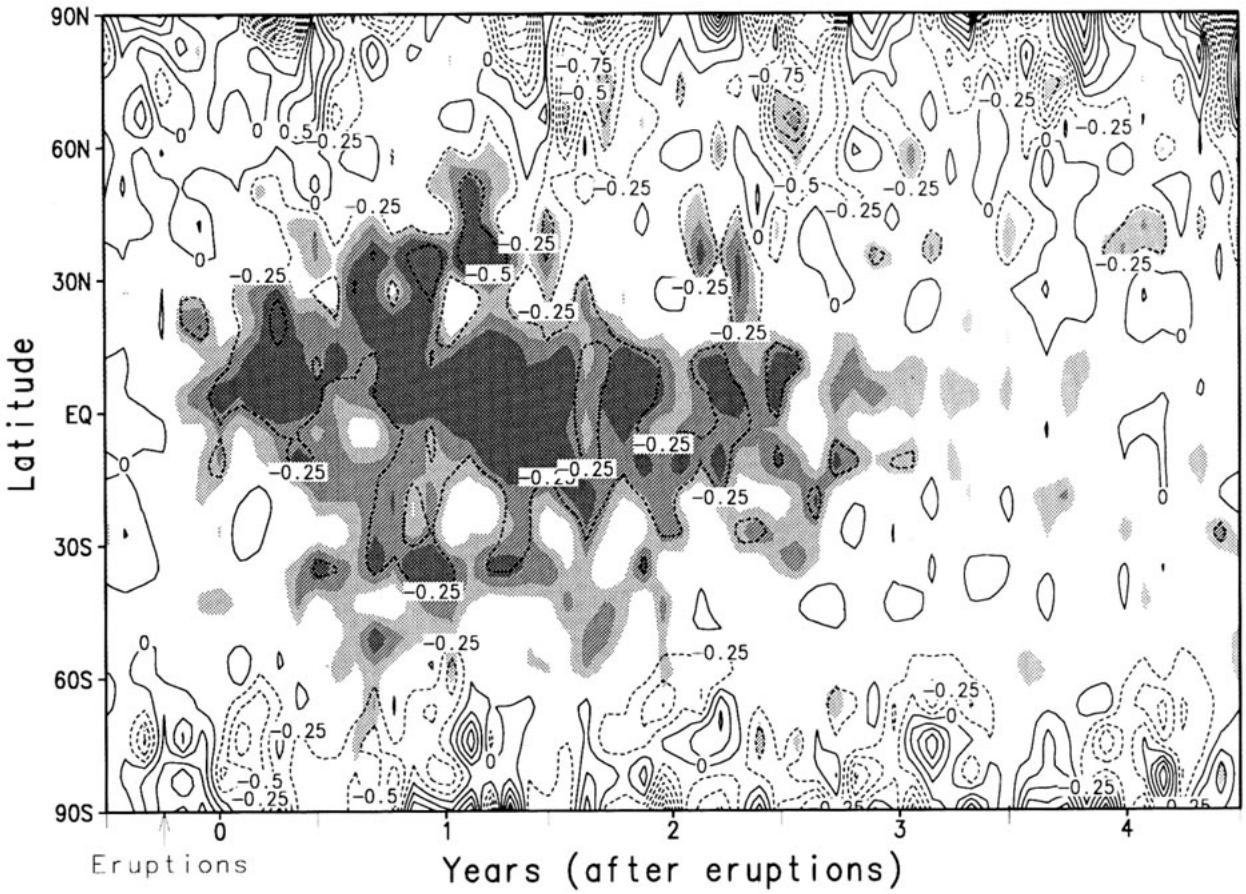

FIG. 5. Zonal average mean temperature anomalies for the average of all volcano cases. Contour interval is 0.25°C. Shading indicates statistical significance from the t test. Lightest shading is significant at the 95% level, medium shading at the 99% level, and darkest shading at the 99.9% level.

cluded the precise determination of long-time scale effects. The same model was used by Hansen et al. (1992) to examine the effects of the 1991 Mt. Pinatubo eruption by running two more volcano cases with scenario B as described below. They showed global and NH midlatitude time series and maps of seasonal mean temperature patterns and discuss the high regional variability.

In this study we extend these results by examining in detail the response of the climate system to volcanic eruptions in the Hansen et al. (1988) GISS transient simulations. We first describe how we extracted the volcanic signal from the GCM output, and then describe the temperature, precipitation, and tropical zonal wind signals.

2. The GISS volcanic signal

The GISS GCM was run with climate forcing of greenhouse gases and stratospheric aerosols from volcanic eruptions for three scenarios (Hansen et al. 1988). In this paper we analyze scenarios A and B of this experiment (Fig. 1). Scenario A assumed that the greenhouse forcing increases exponentially and in scenario B, the greenhouse climate forcing increased by a constant amount annually. Stratospheric aerosols were also added to provide a second climate forcing. Because of the small size (diameter < 1 μm) of long-lived stratospheric aerosols, their effect on planetary albedo exceeded their effect on infrared transmission, resulting in a reduction of net radiation at the tropopause, but heating in the stratosphere.

Details of the stratospheric aerosol distributions are given in appendix B of Hansen et al. (1988). They were based on observations of the 17 March 1963 Agung and the 3 April 1982 El Chichón eruptions, both of which occurred in spring. This allowed us to examine the seasonal cycle of the response in our composite with the initial forcing occurring at the same time of year for all the volcanoes. In both cases, the aerosols stayed in the tropics for about 6 months and then were spread globally. The resulting global radiative forcing was such that it approximately equaled (but in a negative sense) one-quarter

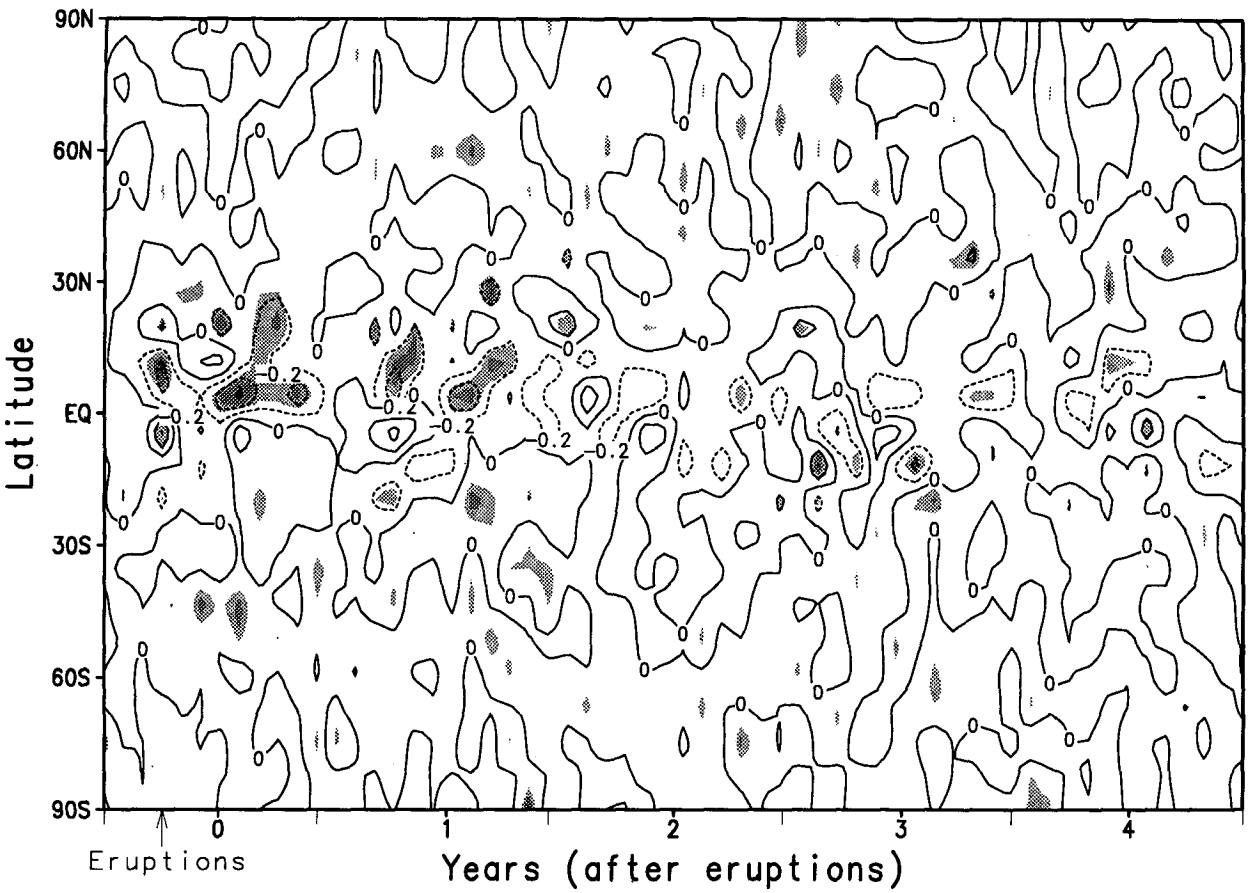

FIG. 6. Zonal average mean precipitation anomalies for the average of all volcano cases. Contour interval is 0.2 mm day^{-1}. Shading as in Fig. 5.

of the positive forcing caused by doubling CO_2. Another way to say this is that each individual eruption produced a negative forcing equal to the positive forcing of all the greenhouse gases added to the atmosphere from 1958 to 1990, but this forcing lasted only about 2 yr.

The simulations were begun in model year 1958 and run into the future. During the period of 1958–1985, the two eruptions of Agung in 1963 and El Chichón in 1982 were added in scenario A and B identically. In scenario B additional large volcanoes were inserted in the year 1995 (identical to El Chichón), in the year 2015 (identical to Agung), and in the year 2025 (identical to El Chichón), while in scenario A no additional volcanic eruptions were included after those from El Chichón decayed to the background stratospheric aerosol level.

We extracted the signals from these seven individual volcanic anomalies in scenario A and B and composited them, in order to remove both the effects of natural variability and greenhouse warming, in the following way. Using monthly average model output, for each point for each month for each parameter, we averaged the parameter for the 3-yr period before the eruption, waited 10 yr, calculated another 3-yr average, and calculated a linear variation between these two 3-yr periods. We then subtracted the actual values for each month during the year of the eruption and the following 9 yr from this linear extrapolation. The key years were the years of the volcanic eruptions in each scenario (1963 and 1982 in scenario A and 1963, 1982, 1995, 2015, and 2025 in scenario B). We then examined the volcanic anomalies for each volcano thus constructed and averaged together all seven cases to further remove natural variations between the seven cases. This procedure assumes that the effect of the volcano lasts less than 10 yr, that a linear variation during a 10-yr period is a valid approximation for the greenhouse warming that would have occurred in the absence of a volcanic eruption, and that a 3-yr average before and after this period is long enough to average out natural variations while short enough to exclude substantial greenhouse-induced changes. The procedure is illustrated for temperature in Fig. 2. The same procedure was used for precipitation and zonal wind.

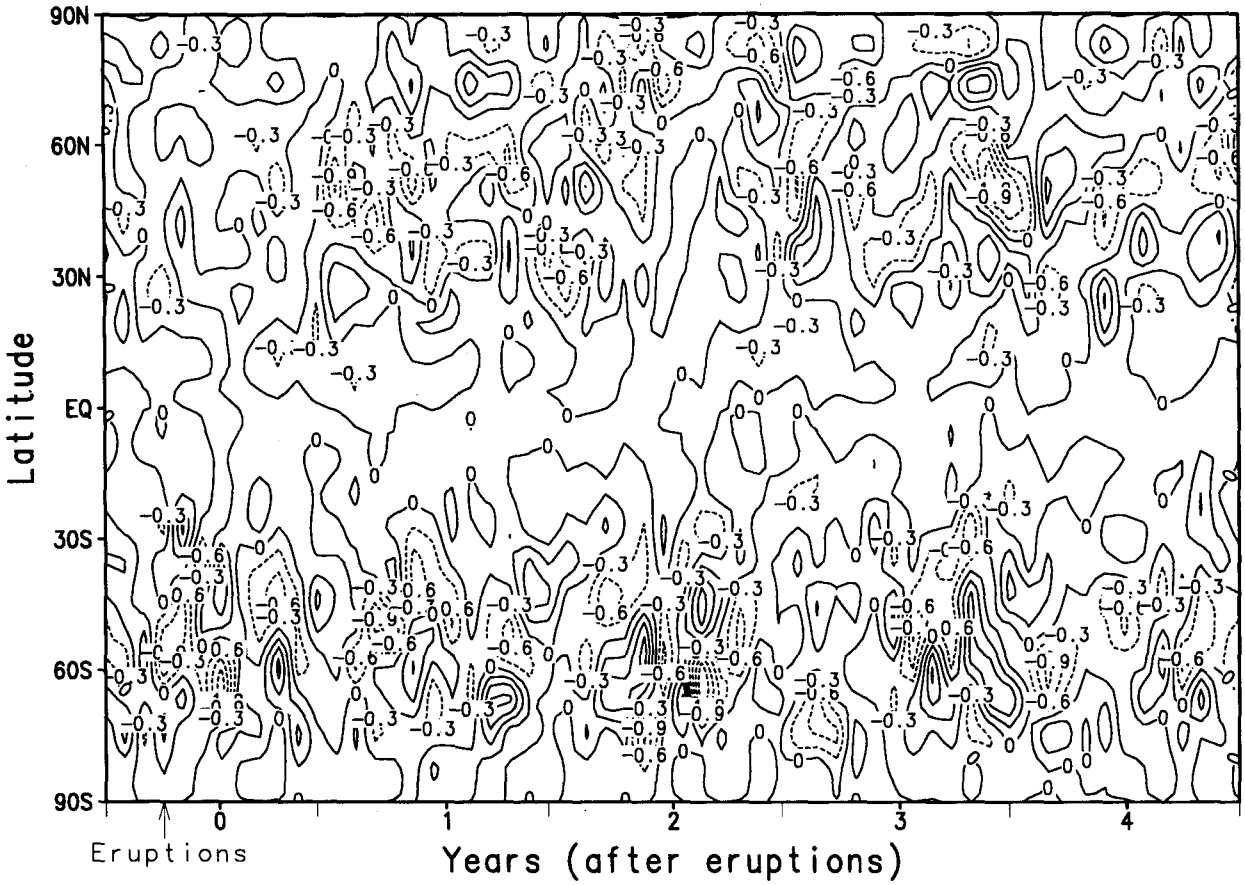

FIG. 7. Zonal mean surface zonal wind anomalies (m s^{-1}) for the average of all volcano cases for the Pacific region (120°E–120°W). Contour interval is 0.3 m s^{-1}.

3. Results

a. Global mean anomalies

Figure 3 shows the global mean anomalies of temperature and precipitation for the seven cases and for the average. The eruptions occurred in the spring of year 0 in each case. After each volcano there is a decrease in temperature and precipitation for several years. The temperature response lasts for more than 4 yr, while the precipitation response can only be seen for 2 or 3 yr. Compared to the interannual standard deviation 0.11°C of the model's global mean for the 100-yr control run, the maximum anomalies due to volcanic eruptions are significant at the level of 5% ($\geq 2\ \sigma$). The anomalies in precipitation are also larger than 2σ ($= 0.03$ mm day^{-1}) of the model's global mean precipitation for the 100-yr control run.

Figure 4 shows that the cooling in the NH is larger than that in the Southern Hemisphere (SH). The largest cooling occurs in the second summer after the eruptions, designated as year 1, since the eruptions occur in year 0. For precipitation, there is not any obvious reduction in the SH, but a large reduction occurs in the NH. This can be explained by the fact that the intertropical convergence zone (ITCZ), where most of the precipitation changes occur (see next section) is mostly north of the equator. Part of the variations shown here are due to north–south movements of the ITCZ, and some are due to precipitation reductions in the ITCZ.

b. Zonal mean anomalies

The zonal mean surface air temperature anomalies averaged for all seven cases are shown in Fig. 5, which also shows the statistical significance of those anomalies as determined by a Student's t-test comparing them to the 100-yr control run of the model that was run with no external forcing. Cooling dominates in the tropical regions for 3 yr after eruptions. This must be the direct effect of volcanic eruptions, since the concentration center of stratospheric aerosols is located in these regions where increased planetary albedo due to stratospheric aerosols reduces solar radiation reaching the surface. Large anomalies also appear in the high latitudes due to the feedback processes between snow and

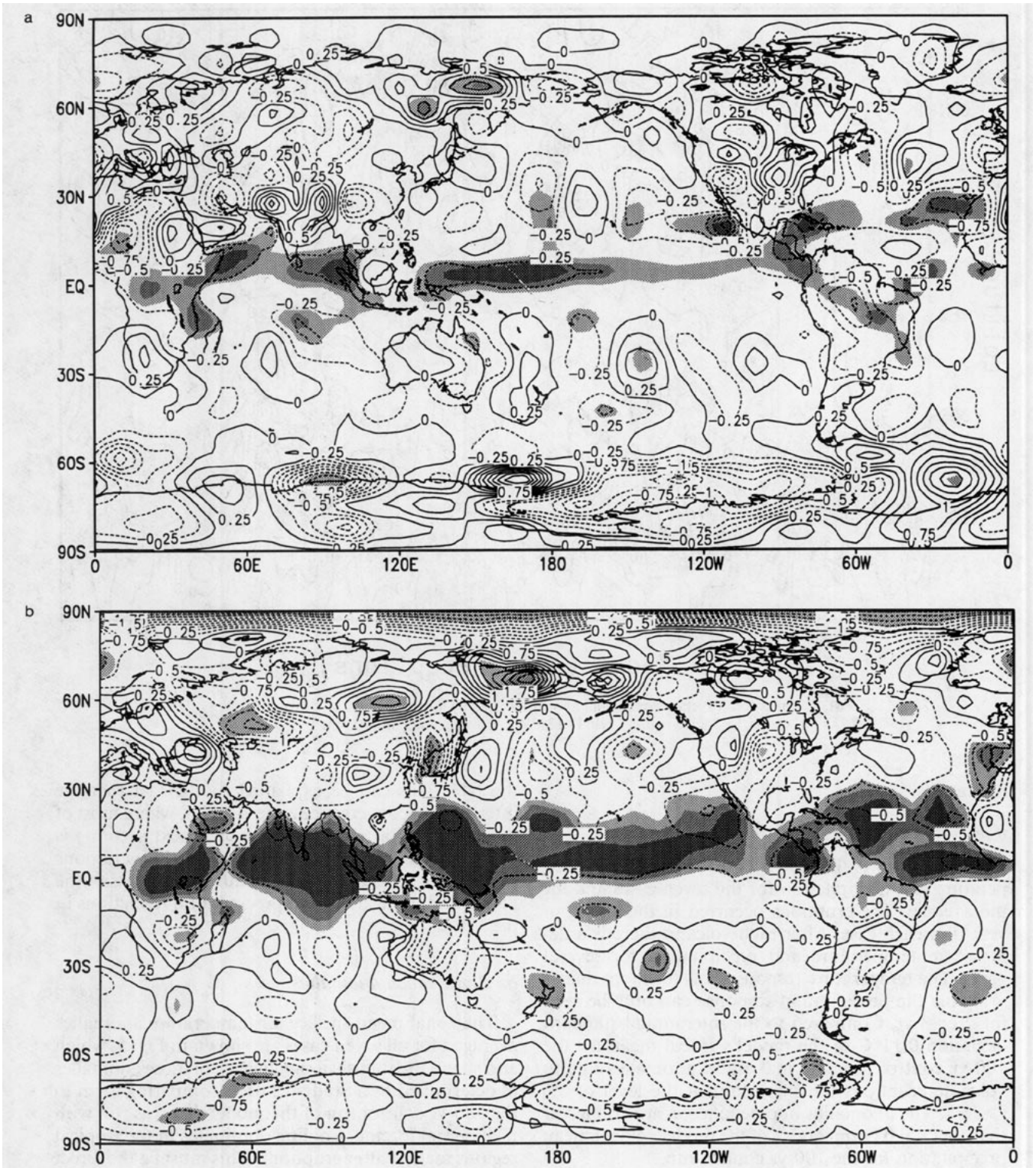

FIG. 8. Global pattern of seasonal-average temperature anomalies (°C) for all the volcanoes, with contour intervals and shading as in Fig. 5. (a) Northern Hemisphere summer (June, July, August), year 0. (b) Fall (SON), year 0. (c) Winter (DJF), year 0–1. (d) Spring (MAM), year 1. (e) Summer (JJA), year 1.

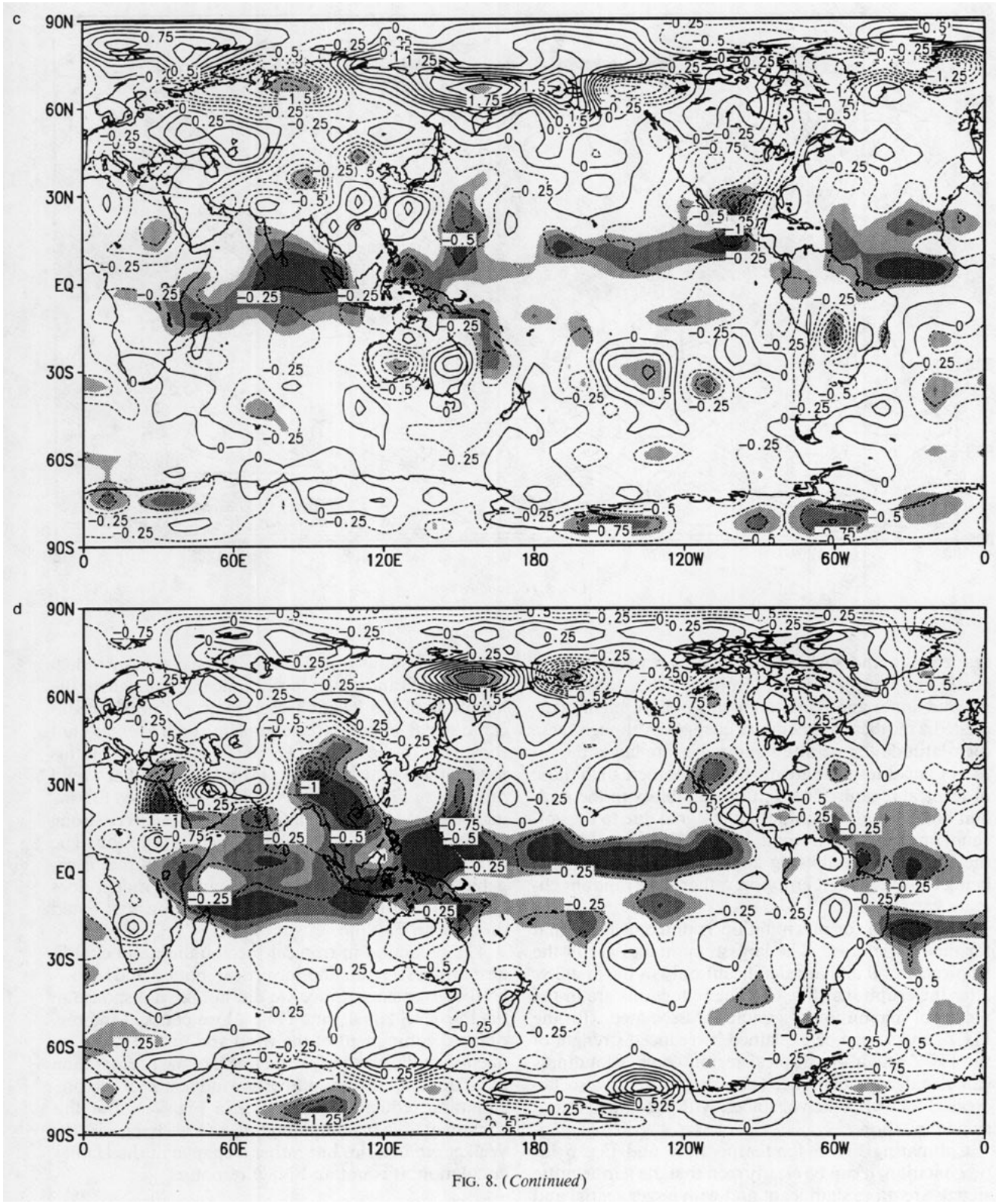

FIG. 8. (*Continued*)

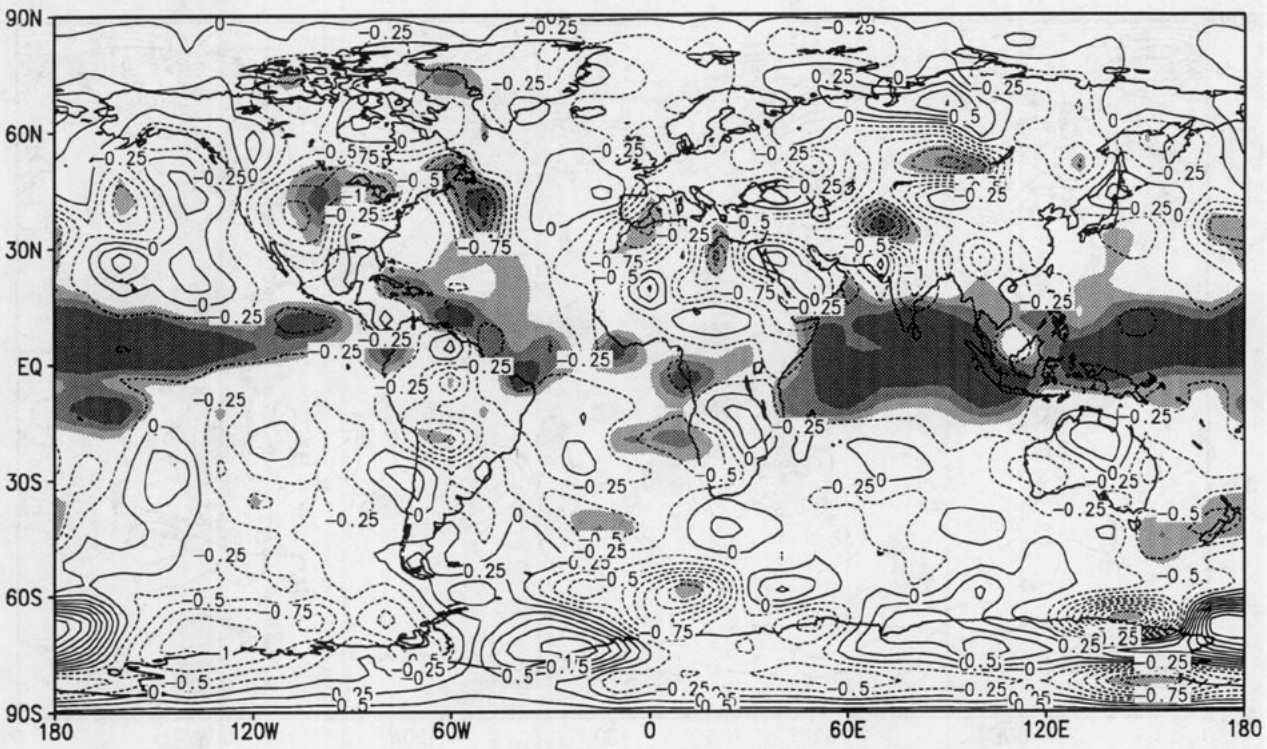

FIG. 8. (*Continued*)

sea ice area and surface albedo, and between sea ice and ocean thermal inertia (Robock 1983, 1984). Sea ice and snow anomalies (not shown) are highly correlated with these temperature changes. Although these high-latitude temperature anomalies are large, the ratios of signal-to-noise are much smaller there than those in tropical regions. The natural variability in the mid- and high latitudes dominates the signal due to the volcano, implying that it would be very difficult to identify the signal there following any individual eruption as being caused by that eruption rather than random climate variations.

The pattern for precipitation is different from that for the temperature. The largest anomalies are in the tropical region and are significant only in the first 2 yr after the eruptions (Fig. 6). The reductions are in the region of maximum precipitation associated with the ITCZ, and so can be explained by reduced strength of the ITCZ when the tropical region cools. Cloudiness calculated by the model (not shown here) also decreased following the volcanoes, with the same pattern as precipitation.

Comparing Fig. 5 for temperature and Fig. 6 for precipitation, it can be clearly seen that the temperature signals are more significant and with larger spatial and temporal scales. This is what we expect from our understanding of the typical scales of the physical processes responsible for temperature and precipitation changes in the climate system.

Figure 7 shows zonal mean, surface zonal wind (u component) anomalies for the volcanic average for the longitude of the Pacific Ocean. There is no clear volcanic signal, either in the complete zonal average (not shown) or in the tropical Pacific (Fig. 7). Thus, in this model, there is no evidence of wind changes that would produce an ENSO event, as had been suggested following the great 1982–83 ENSO, which became very strong in the months just after the El Chichón eruption. The GISS GCM does not have an ocean model that is capable of producing an El Niño, but this model does not even produce atmospheric circulation that could produce an El Niño.

The reduction in tropical precipitation and cloudiness implies a reduction in vertical motion and in low-level convergence. Since we did not see a response in the low-level zonal wind (Fig. 7) we checked the meridional component of the wind and indeed saw a reduction of the northerly wind north of the precipitation reduction and of the southerly wind south of the precipitation reduction (as shown in Fig. 9a). But this consistent dynamical change is not a change in the Walker circulation, but rather a change in the Hadley circulation; it is not an ENSO response.

c. Seasonal mean anomaly maps

The temperature anomalies and their significance for the first seasonal cycle after the eruptions are shown

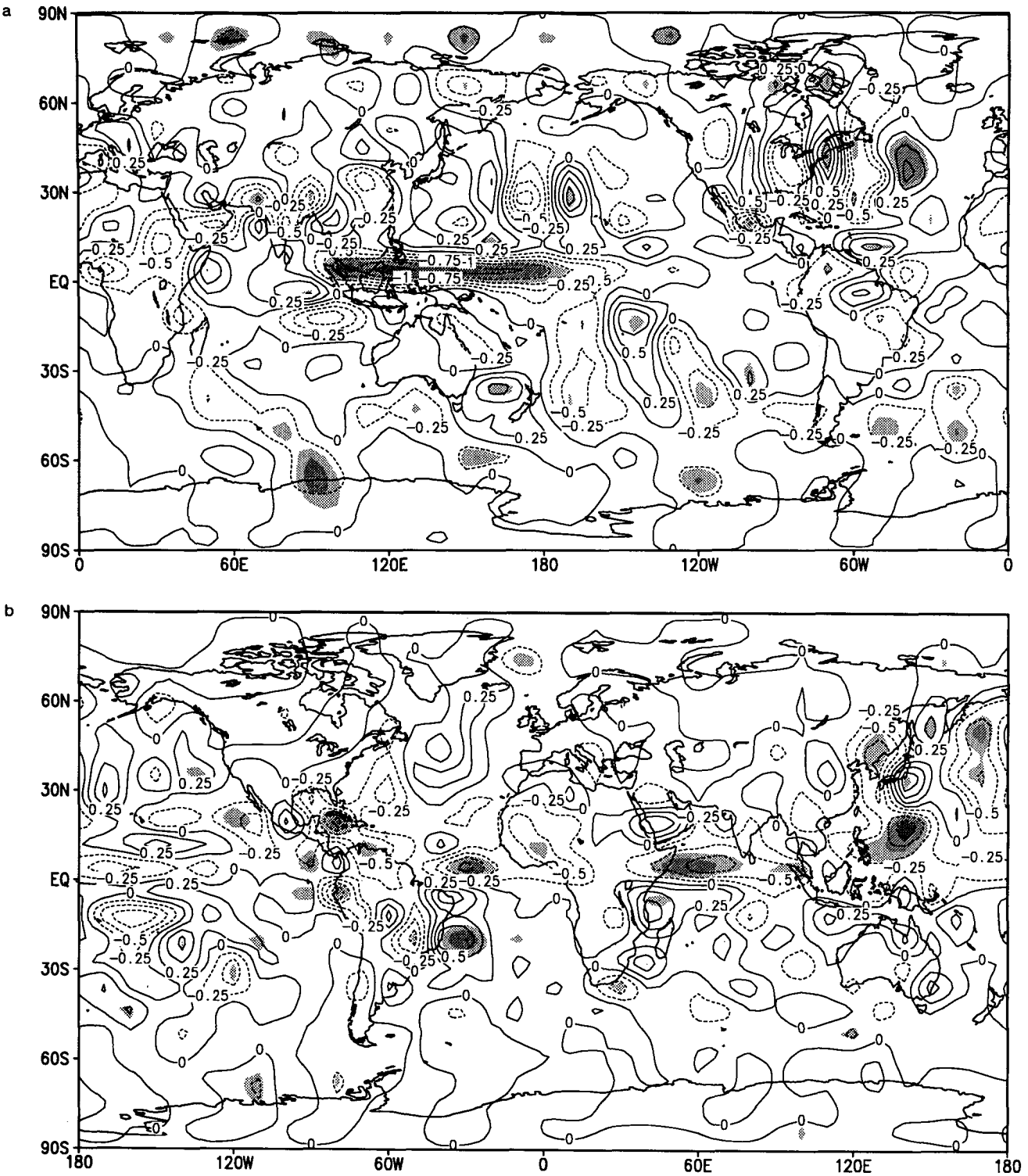

FIG. 9. Global pattern of seasonal-average precipitation anomalies (mm day^{-1}) for all the volcanoes, with contour intervals and shading as in Fig. 7. (a) Northern Hemisphere summer (June, July, August), year 0. (b) Fall (SON), year 0.

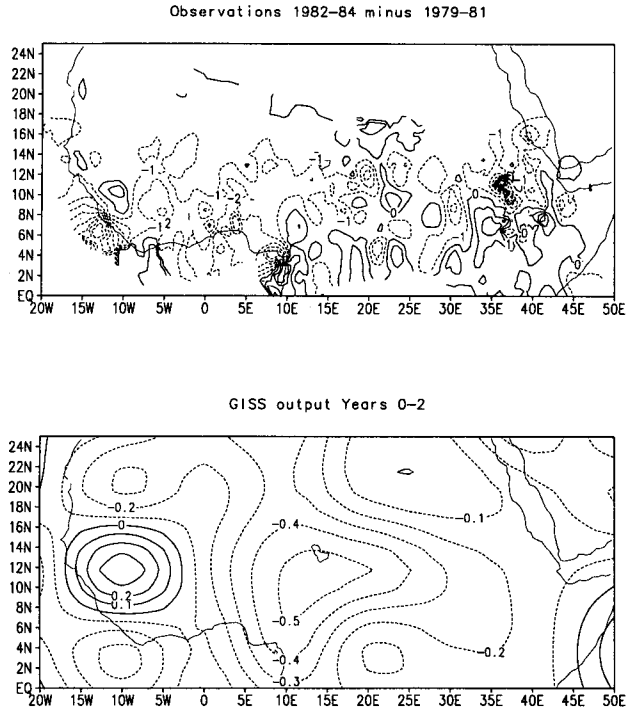

FIG. 10. Patterns of rainy season (JJAS) precipitation changes over northern Africa (mm day^{-1}). Top: observations of 1982–1984 minus the same months for 1979–1981. Bottom: average for years 0, 1, and 2 after the volcanic eruptions.

in Fig. 8. A pattern of cooling is found for all seasons in the tropics with the largest cooling in the second summer (year 1). There are large temperature anomalies in the higher latitudes but with less significance. In particular, in the first winter after the eruptions (Fig. 8c), areas of warming are seen over Canada and Europe, with cooling over the mideast and northern Africa, in agreement with observations composited for the 12 largest eruptions since 1883 (Robock and Mao 1992) and perpetual January GCM results (Graf et al. 1994). In the second summer after the eruptions (Fig. 8e), significant cooling is seen over most of North America.

The occurrence of the largest volcanic signal in precisely the same location as the largest signal during ENSO events presents a challenge to the climatologist to extract these signals from the climatic record when both are occurring at the same time, such as the recent examples of 1982–83 after El Chichón and 1991–92 after Pinatubo. Angell (1988, 1990) and Quiroz (1983) have attempted this for surface and stratospheric temperatures on a large scale. They were successful because the volcanic signal has a longer time scale, lasting for several years, while the ENSO warm event is typically over in just one year. The largest volcanic signal occurs more than one year after the eruption, when the ENSO signal would have dissipated if the ENSO event and the volcano occurred simultaneously. Robock and Mao (1994) demonstrate this on a geographically specific basis.

Large precipitation anomalies are also found in the tropical regions (Fig. 9). Although not significant, the NH summer pattern of precipitation is particularly striking, in that a very large reduction occurs along the equatorial Pacific (Fig. 9a). This pattern is contrary to the ENSO pattern, in which precipitation increases in the equatorial region centered on 180° longitude. The pattern for March through May of year 1 (not shown) looks like a shift of the ITCZ southward. But all the precipitation patterns are much less homogeneous in time and space than the temperature signals (Fig. 8).

There is also a striking, but not significant, precipitation reduction in northern Africa. When one looks at the data on African rainfall, the lowest rainfall amount in the Sahel region for the period 1940–1990 was during the summers of 1982–84, which were just after the El Chichón eruption, the largest eruption of this time period. Figure 10 shows the rainfall pattern for these years as compared to the three years before the eruption (1979–1981), in the same manner as the model anomalies were calculated, compared to the average precipitation for years 0, 1, and 2 for the seven volcano cases. Although not proof, this suggests that Sahel drought may be enhanced by large tropical eruptions.

4. Discussion and conclusions

The GISS GCM transient run (Hansen et al. 1988) provides an opportunity to examine the GCM signal of typical tropical volcanic eruptions. The most significant signals of both temperature and precipitation are in the tropics over the ocean. The conventional wisdom that the oceans respond more slowly than the land to forcing, and that we must search for signals of climate change over land is challenged by this finding. This GCM uses a mixed-layer ocean, which on the one-year time scale found here is not different from any other ocean models that include slow deep currents, but the interannual variability of the SST in this GCM is less than observed. The temperature changes are not large, and are within our experience of the seasonal cycle of temperatures over oceans, even in the tropics, and the low variability allows detection of the signal. The peak responses are in the same region that is the center of ENSO cycle activity. However, the volcanic signals, at least in temperature, are larger scale in time and space, so that examination of temperatures in the subtropics during ENSO events, and in the tropics before and after ENSO events, will help meet the challenge in the future to separate out these signals as the events are occurring.

Acknowledgments. We thank Jim Hansen and David Rind for valuable discussions, Roy Jenne and Dennis Joseph at NCAR for providing the GISS model output, Graham Farmer for precipitation data, and Brian Doty

for development and enhancements of the GrADS plotting software, which was used for all the figures. This work was supported by NSF Grant ATM 89-20590 and NASA Grant NAG 5-1835.

REFERENCES

Angell, J. K., 1988: Impact of El Niño on the delineation of tropospheric cooling due to volcanic eruptions, *J. Geophys. Res.*, **93,** 3697–3704.

——, 1990: Variation in global tropospheric temperature after adjustment for the El Niño influence, 1958–89. *Geophys. Res. Lett.*, **17,** 1093–1096.

Asaturov, M. L., M. I. Budyko, K. Ya. Vinnikov, P. Ya. Groisman, A. S. Kabanov, I. L. Karol, M. P. Kolomeev, Z. I. Pivovarova, E. V. Rozanov, and S. S. Khmelevtsov, 1986: *Volcanics, Stratospheric Aerosol and Earth's Climate* (in Russian). Gidrometeoizdat, 256 pp.

Ellsaesser, H. W., 1983: Isolating the climatogenic effects of volcanoes. UCRL-89161, Lawrence Livermore National Laboratory, Livermore, CA, 29 pp.

Franklin, B., 1784: Meteorological imaginations and conjectures. *Manchester Literary and Philosophical Society Memoirs and Proceedings,* **2,** 122.

Graf, H.-F., I. Kirchner, R. Sausen, S. Schubert, 1992: The impact of upper-tropospheric aerosol on global atmospheric circulation, *Ann. Geophys.*, **10,** 698–707.

——, ——, A. Robock, and I. Schult, 1994: Pinatubo eruption winter climate effects: Model versus observations. *Climate Dyn.*, in press.

Hansen, J., I. Fung, A. Lacis, D. Rind, S. Lebedeff, R. Ruedy, G. Russell, and P. Stone, 1988: Global climate changes as forecast by the GISS 3-D model. *J. Geophys. Res.*, **93,** 9341–9364.

——, ——, R. Ruedy, and M. Sato, 1992: Potential climate impact of Mount Pinatubo eruption. *Geophys. Res. Lett.*, **19,** 215–218.

Hirono, M., 1988: On the trigger of El Niño Southern Oscillation by the forcing of early El Chichón volcanic aerosols. *J. Geophys. Res.*, **93,** 5365–5384.

Hunt, B. G., 1977: A simulation of the possible consequences of a volcanic eruption on the general circulation of the atmosphere. *Mon. Wea. Rev.*, **105,** 247–260.

Kondratyev, K. Ya., 1988: Volcanoes and Climate. WCP-54, WMO/TD-No. 166, World Meteorological Organization, Geneva, 103 pp.

Lamb, H. H., 1970: Volcanic dust in the atmosphere; with a chronology and assessment of its meteorological significance. *Philos. Trans. Roy. Soc. London,* **A266,** 424–533.

Pollack, J. B., D. Rind, A. Lacis, J. E. Hansen, M. Sato, and R. Ruedy, 1993: GCM simulations of volcanic aerosol forcing. Part I: Climate changes induced by steady state perturbations. *J. Clim.*, **6,** 1719–1742.

Quiroz, R. S., 1983: The isolation of stratospheric temperature change due to the El Chichón volcanic eruption from nonvolcanic signals. *J. Geophys. Res.*, **88,** 6773–6780.

Rind, D., N. K. Balachandran, and R. Suozzo, 1992: Climate change and the middle atmosphere. Part II: The impact of volcanic aerosols. *J. Climate,* **5,** 189–208.

Robock, A., 1983: Ice and snow feedbacks and the latitudinal and seasonal distribution of climate sensitivity. *J. Atmos. Sci.*, **40,** 986–997.

——, 1984: Climate model simulations of the effects of the El Chichón eruption. *Geofis. Int.*, **23,** 403–414.

——, 1991: The volcanic contribution to climate change of the past 100 years. *Greenhouse-Gas-Induced Climatic Change: A Critical Appraisal of Simulations and Observations,* Michael E. Schlesinger, Ed., Elsevier, 429–444.

——, and J. Mao, 1992: Winter warming from large volcanic eruptions. *Geophys. Res. Lett.*, **19,** 2405–2408.

——, ——, 1994: The volcanic signal in surface temperature observations. *J. Climate,* **7,** submitted.

Toon, O. B., 1982: Volcanoes and climate. *Atmospheric Effects and Potential Climatic Impact of the 1980 Eruptions of Mount St. Helens,* Adarsh Deepak, Ed., NASA Conference Publication 2240, NASA, 15–36.

——, and James B. Pollack, 1980: Atmospheric aerosols and climate. *Am. Sci.*, **68,** 268–278.